IEEE Access
Multidisciplinary | Rapid Review | Open Access Journal

Received 2 November 2023, accepted 19 November 2023, date of publication 30 November 2023,
date of current version 8 December 2023.

Digital Object Identifier 10.1109/ACCESS.2023.3338145

RESEARCH ARTICLE

QuCardio: Application of Quantum Machine Learning for Detection of Cardiovascular Diseases

SHARANYA PRABHU[1], SHOURYA GUPTA[1], GAUTHAM MANURU PRABHU[1], AARUSHI VISHAL DHANUKA[2], AND K. VIVEKANANDA BHAT[1], (Senior Member, IEEE)

[1]Department of Computer Science and Engineering, Manipal Institute of Technology, Manipal Academy of Higher Education, Manipal, Karnataka 576104, India
[2]Department of Information and Communication Technology, Manipal Institute of Technology, Manipal Academy of Higher Education, Manipal, Karnataka 576104, India

Corresponding author: K. Vivekananda Bhat (kv.bhat@manipal.edu)

This work was supported in part by the Ministry of Electronics and Information Technology (MeitY), Quantum Computing Applications Laboratory (QCAL), Government of India, to access Braket-a quantum computing facility through Amazon Web Services (AWS) Cloud; and in part by the Manipal Academy of Higher Education, Manipal, India.

ABSTRACT This research is the first of its kind to leverage the power of Quantum Machine Learning (QML) to perform multi-class classification of Cardiovascular Diseases (CVDs). We propose a novel approach that enables multi-class classification with Pegasos Quantum Support Vector Classifier (QSVC). The QSVC and the Pegasos QSVC significantly outperform the classical SVC by a margin of +10.76% and +9.72%, respectively. The paper further ventures into a quantum deep learning based architecture with a novel Quanvolutional Neural Network (QNN) implementation, outperforming not only its classical CNN counterpart by +3.88% but also the other models by achieving 97.31% accuracy, 97.41% precision, 97.31% recall, 97.30% F1 score, and 99.10% specificity.

INDEX TERMS Quantum machine learning (QML), quantum support vector machine (QSVM), Pegasos, quanvolutional neural network (QNN), medical image classification, cardiovascular disease classification.

I. INTRODUCTION

Cardiovascular diseases (CVDs), one of the largest causes and concerns of mortality and disability in the world [1], refers to a group of illnesses that affect the heart muscles. In 2020, approximately 19 million deaths were found to be caused by CVD globally. This increase was about 18.7% higher than in 2010. Some examples of CVDs include myocardial infarction, arrhythmia, stroke, and coronary artery disease. They are frequently brought on by a confluence of risk factors comprising smoking, high blood pressure, high cholesterol, obesity, chronic inactivity, and a family history of the disease.

Early detection of CVDs has been done by utilizing advances in the field of biotechnology. Major developments in the biosensors domain, such as the advent of lab-on-a-chip technology, have demonstrated the ability to detect cardiac markers [2]. Advances in microfluidics technology have helped reduce application time and integrate multiple clinical assays into a single device [3]. Protein chip development has also significantly contributed to early CVD detection [4].

The past two decades have witnessed a remarkable advent of Artificial Intelligence (AI), Natural Language Processing (NLP), Computer Vision (CV), and other areas and domains such as healthcare, and cybersecurity. Machine learning algorithms have achieved unprecedented accomplishments due to the availability of vast data aggregates. AI research for CVDs can be broadly summarised into Machine Learning (ML), Deep Learning (DL), unsupervised learning, Artificial Neural Networks (ANNs), and Convolutional Neural Networks (CNNs) [5].

A comparison of computational intelligence approaches for the classification of cardiac diseases has been provided by [6]. The paper presents seven approaches, namely, Decision Trees (DT), K-Nearest Neighbors (KNN), Support Vector Machines (SVM), Deep Neural Networks (DNN), Random Forests (RF), Logistic Regression (LR), and Naive Bayes (NB). The effectiveness of each strategy is assessed

The associate editor coordinating the review of this manuscript and approving it for publication was Yiming Tang.

using standard datasets. Their research has shown that the DNN achieves 98.15% accuracy, which is comparatively superior to the other methods.

The high cost of computation is the primary disadvantage of AI techniques [7]. The advantage of Quantum Computing (QC) methods, on the other hand, is that they can accelerate computation by applying the principles of quantum mechanics. Quantum computers are structured on probabilistic results dependent on intrinsically coupled quantum systems [8]. This results in a massive increase in parallel computations due to the superposition of quantum states. Thus, by procedural utilization of fundamental quantum effects such as superposition, interference, and quantum entanglement, quantum algorithms can efficiently circumvent the drawbacks faced in classical AI techniques [9]. Differences between classical ML and QML have been reviewed in [10].

QC has been explored in solving complex sampling tasks that require expensive computations on classical computing systems to establish quantum supremacy in the near-term [11]. An essential task in QC involves finding appropriate use cases and applications where a quantum computer or a quantum computational mechanism can dispense a substantial speedup. Various QC approaches have been employed in the domains of healthcare [10], financial risk analysis [11], portfolio management and optimization [12], and trading algorithms development [13] to solve real-world problems.

The Noisy Intermediate-Scale Quantum (NISQ) period, the current QC era, explains the present state of QC technology. Quantum computers are becoming increasingly powerful and effective. However, they are still susceptible to errors such as noise, hardware shortcomings, and decoherence [14]. Nonetheless, significant advancements in the field prospects do look promising.

A. PRELIMINARIES AND NOTATIONS

This section aims to introduce some mathematical notations useful in quantum computing. The Ket notation $|\psi\rangle$ represents an object as a column vector. The complex conjugate of a ket is called the bra. Hence it is collectively termed the ''Braket'' notation.

A single qubit represents a two-level quantum system in a two-dimensional Hilbert space C^2 with orthonormal bases. It can be described using the superposition principle:

$$|\psi\rangle = \alpha|0\rangle + \beta|1\rangle$$

Here, $|\psi\rangle$ is a linear combination of the quantum states of two basis states $|0\rangle$ and $|1\rangle$ that expresses the quantum state of a qubit, α and β are complex coefficients that represent the probability amplitudes of the two states, respectively. Table 1 summarizes the common quantum operations performed on qubits.

B. MOTIVATION AND CONTRIBUTIONS

The Quantum Machine Learning (QML) models presented in this paper use supervised multiclass classification and are employed to detect various CVDs using Electrocardiogram (ECG) images. Hyperparameters of the models used are tuned to get the most optimal results, and the final results procured from each model are described.

The motivation behind our work follows along with the advent of machine learning coupled with quantum computing to explore the growing field of QML and establish better results in the field of medical image classification. Owing to resource constraints in image processing, the progression in performance, albeit notable, isn't fully optimal yet. Our research aims to benchmark QML models for CVD classification using ECG images, which, to the best of our knowledge, has not been done thus far. We aim to explore Support Vector Classifier (SVC) based and DL-based techniques to improve the performance measured against the classical counterpart. We also intend to facilitate multi-class classification with Pegasos Quantum SVC (QSVC) using a mathematical combination of its binary classification models.

The main contributions of our study can be summarized in the following points.

1) Cardiovascular disease classification problem on ECG images has been explored using three Quantum Machine Learning models.
2) The QSVC model has significantly outperformed its classical counterpart, the SVC model, by +10.76% accuracy, +9.73% precision, +10.76% recall, +10.79% F1 score, and +3.73% specificity.
3) The Pegasos QSVC, a quantum-enhanced SVM algorithm, presently supports binary classification. A novel workflow has been established to extend its binary classification abilities to perform multiclass classification for four classes.
4) A new architecture for the implementation of Quanvolutional Neural Network (QNN) is proposed.

The remaining sections in the paper have been described here. Section II provides a literature review on QML approaches on medical image classification and QML approaches on cardiac datasets. Section III focuses on the experiment, describing the experimental setup and the dataset used. Furthermore, pre-processing done on the dataset is described here. Subsequently, Section IV explains the three models implemented and the architecture used. Section V focuses on results and discussion of the proposed models. Section VI comprises the conclusion and future scope.

II. LITERATURE REVIEW

Since Feynman first suggested using quantum systems to perform computation in 1982, the field has advanced significantly. The utilization of various quantum systems by multiple organizations, such as superconducting qubits (used by IBM, Google, and USTC), trapped ions (IonQ), and Rydberg atoms (QuEra), acts as the base for promising quantum computers ([15]).

TABLE 1. Common quantum gates and their operations.

Quantum Gate	Notation	Matrix formula	Operation
Pauli-X	$\mathbf{X}$	$\begin{pmatrix} 0 & 1 \\ 1 & 0 \end{pmatrix}$	Bit-flip
Pauli-Y	$\mathbf{Y}$	$\begin{pmatrix} 0 & -i \\ i & 0 \end{pmatrix}$	Bit-flip and Phase-flip
Pauli-Z	$\mathbf{Z}$	$\begin{pmatrix} 1 & 0 \\ 0 & -1 \end{pmatrix}$	Phase-flip
Hadamard	$\mathbf{H}$	$\frac{1}{\sqrt{2}}\begin{pmatrix} 1 & 1 \\ 1 & -1 \end{pmatrix}$	Introduces superposition
Controlled NOT	$\mathbf{CNOT}$	$\begin{pmatrix} 1 & 0 & 0 & 0 \\ 0 & 1 & 0 & 0 \\ 0 & 0 & 0 & 1 \\ 0 & 0 & 1 & 0 \end{pmatrix}$	Conditional Bit-flip
R-X	$\mathbf{RX}$	$\begin{pmatrix} \cos(\frac{\theta}{2}) & -i\sin(\frac{\theta}{2}) \\ -i\sin(\frac{\theta}{2}) & \cos(\frac{\theta}{2}) \end{pmatrix}$	Rotation of θ about X axis
R-Y	$\mathbf{RY}$	$\begin{pmatrix} \cos(\frac{\theta}{2}) & -\sin(\frac{\theta}{2}) \\ \sin(\frac{\theta}{2}) & \cos(\frac{\theta}{2}) \end{pmatrix}$	Rotation of θ about Y axis
R-Z	$\mathbf{RZ}$	$\begin{pmatrix} e^{-i\frac{\theta}{2}} & 0 \\ 0 & e^{i\frac{\theta}{2}} \end{pmatrix}$	Rotation of θ about Z axis

A. APPLICATION OF QML ON MEDICAL DATASETS

Works [16] and [17] compared pertinent quantum neural network architectures, explained their designs, outlined their features, and offered background information. The benchmarked quantum neural Network on the MedMNIST dataset for medical images, specifically the PneumoniaMNIST and RetinaMNIST is given in [18]. The work [19] described generative models using QML techniques. They proved that their algorithm can represent probability distributions better than classical generative models. The development of Variational Quantum Eigensolver (VQE) [20] proliferated advancements in near-term algorithmic systems, further enhancing variational quantum algorithms. The paper notes that the model probability distributions are comparable with classical generative models and that there is an exponential speedup in learning and inference.

The application of QML in radiological image classification is explained in [21]. The authors compared their implementation of the Quantum Classical Convolutional Neural Networks (QCCNN) with the Classical CNN. The results obtained during classification were similar for both cases. The datasets selected were the BreastMNIST and the OrganAMNIST. The paper showed that their QCCNN had overfit. Using two approaches, [22] employed QML techniques for breast cancer detection. The first involved using the quantum genetic algorithm. The second approach consisted of training SVMs on simulated pictures to aid it in recognizing breast cancer edges.

The QML approach introduced by [23] proved to be promising in classifying COVID-19 traits. The quantum neural network was applied to the X-ray scans of Indian COVID-19 patients. The improvement in accuracy compared to a 2D CNN model was observed to be +2.92%. The training time was significantly reduced with quantum-optimized hardware. This further shows the effectiveness of the whole system to scale classification models. The work in [24] developed the QML method to categorize and identify COVID-19 patients. They used the data and the VQC algorithm on several popular QC systems. Their results showed that the classical computers achieved an accuracy of 90%, whereas the quantum computers outperformed their classical counterparts with an accuracy ranging from 94-100%.

The authors in [25] implemented an exploratory data analysis (EDA), a pre-processing approach for data scaling, and the VQC, Root Mean Squared Propagation (RMSprop), and DL models for classification using the PIMA diabetic dataset. In the study, they evaluated RMSprop using the VQC technique and back-propagation and beat the state-of-the-art performance. The research work in [26] extensively summarized the applications of QML in the biomedical domain. The work in [27] has conducted an exhaustive study on the applications of QML in medical imaging.

B. APPLICATION OF QML ON CARDIAC DATASETS

The QML approaches have been employed on multiple standard datasets of cardiac diseases. They include Quantum Random Forest Classifier (QRFC), Quantum K-Nearest Neighbors (QKNN), Quantum SVM (QSVM), Bagging-QSVC, QNN, instance-based QML, Quantum K-means

(Q K-means), and Hybrid Quantum Machine Learning Perceptron (HQMLP). Techniques implemented on the UCI repository are described in [28], [29], [30], [31], and [32]. The researchers in [28] use a QRFC using the Euclidean distance metric. The work in [29] employed a QKNN-based approach after performing standard data preprocessing techniques, including Principal component analysis (PCA), min-max scaling, and outlier rejection. The authors in [30] observed that the Bagging QSVC outperformed QSVC, QNN, and QVC. In [31] compared an SVM and a QSVM on the dataset and observed that the QSVM showed better accuracy with lower time complexity. The method uses an optimized QSVM and a hybrid quantum multi-layer perceptron. The quantum K-means clustering approach has been described in [29] with distance calculation performed using the swap test circuit. The QNN proposed in [32] achieved a high accuracy on the Cleveland dataset. The authors in [33] developed an HQMLP model to predict ischemic heart disease by considering 10 features.

III. EXPERIMENTAL SETUP

On a computer having the following specifications: x86-64 architecture with 4 CPU cores and 2 threads per core, featuring an Intel(R) Xeon(R) CPU @ 2.20GHz and equipped with 30GB of RAM, the experiments were carried out.

A. ECG IMAGES DATASET OF CARDIAC PATIENTS

For this research, 928 ECG images of cardiac patients from a dataset by the Ch. Pervaiz Elahi Institute of Cardiology in Multan, Pakistan [34] was considered. The dataset under consideration consists of four classes, namely, *Normal Person (NP), Abnormal Heartbeat (AH), Myocardial Infarction (MI),* and *History of Myocardial Infarction (H. MI)*. The data split is 284, 233, 240, and 172 images, respectively.

The class represented as *NP* illustrates people having no cardiac abnormalities. *AH* class refers to patients suffering from Cardiac Arrhythmia. This indicates a deviation from the regular heartbeat's rhythm or pace [35]. The condition arises when the electrical impulses controlling the heartbeats are coordinated improperly. This results in the heart beating quickly (tachycardia), too slowly (bradycardia), or irregularly.

The *MI*, also known as a heart attack [36], is a medical emergency that occurs when blood supply to a portion of the heart muscle is cut off, typically due to an accumulation of fatty deposits in the coronary arteries. The chest discomfort, loss of breath, and other symptoms may result from this, harming or killing the heart muscle. If not treated quickly and efficiently, this can result in significant consequences such as heart failure, arrhythmia, and sudden cardiac death. The *H. MI* refers to individuals who have just experienced recovery from a myocardial infarction.

In the proposed approaches to the classification task, the dataset has been split into train and test sets in the ratio of 80:20. The Fig. 1 represents sample images from each class of the dataset.

B. DATA PREPROCESSING

The edges of all the images in the dataset are cropped out to retain only the portion occupied by the region of interest, specifically the ECG graph. The background removal was performed by thresholding pixel values resulting in a binary image. The ECG wave readings in the foreground were represented in black, and the background in white. Vertical lines, common to all images indicating the separation between the lead readings, were also removed. These pre-processed images are further used for all the experiments. Fig. 2 showcases an ECG image from class *NP* after the pre-processing stages.

IV. METHODOLOGY

A. QUANTUM SUPPORT VECTOR CLASSIFIER (QSVC)

A QSVC [37] is the quantum equivalent of the classical SVC [38] or SVM. The SVC is a supervised machine learning model that solves classification problems and requires high computational resources due to operations in a high dimensional space. It functions by identifying a line or a hyperplane to separate two groups or classes and applies one vs. one or one vs. rest methods to handle multi-class classification tasks. The classical SVC applies kernels, which are complex mappings that add new dimensions to the data, hence constructing higher-dimensional feature spaces. These mappings ease boundary identification, thus separating the classes. One the other hand, the QSVC employs a quantum kernel to capture more complex similarities between data points that cannot be efficiently computed with normal kernels. Additionally, it can reduce the number of classical computations required for SVC, leading to faster and more efficient classification.

1) FEATURE EXTRACTION

Pre-trained DNNs support transfer learning and facilitate efficient feature extraction from images. These neural networks have been trained on massive datasets comprising of more than a million images belonging to hundreds of classes.

In the proposed implementation, the images have been resized to 340 × 340 to handle computational capacity limitations and speed up processing. A ResNet50 model [39] has been employed to the dataset in order to extract the features. The model weights have been initialized with pre-trained weights on the Imagenet dataset [40]. The image features are extracted from the *pool1_pool* layer. This layer is a max-pooling layer that takes the maximum of a set of values within a kernel window and outputs it as the new value for the corresponding location. This is a shallow-level layer containing more low-level features. The extracted features of all images are flattened into a one dimensional feature vector and subsequently stacked together to form a feature matrix. Dimensionality of the obtained feature matrix is reduced using Truncated Singular Value Decomposition (SVD) [41]. This technique is applied such that it yields the top 9 most

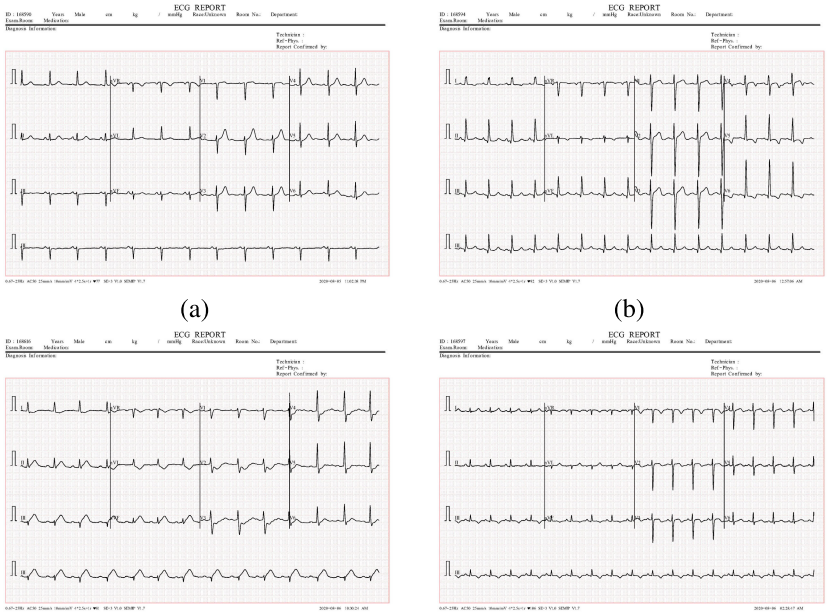

FIGURE 1. Sample images from the dataset (a) NP (b) AH (c) MI (d) H. MI.

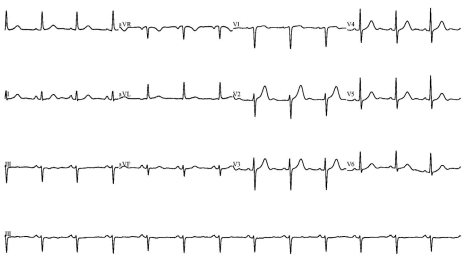

FIGURE 2. Preprocessed version of Fig. 1(a).

relevant features from the images. Furthermore, the feature matrix is scaled to a range of 0 to 1, thus enforcing uniformity.

2) ALGORITHM

The QSVC algorithm as outlined in Fig. 3 can be summarized into four significant steps:

1) Encoding of data: The input classical data $\vec{x}$ in quantum states is encoded using a quantum feature map $\phi(\vec{x})$. In a complex Hilbert space, the encoded data can be represented by a unit vector.
2) Quantum Kernel Computation: A quantum circuit is used to compute a mathematical function known as a quantum kernel that assesses the similarity or inner product between two encoded data points in the feature space.
3) Quantum Optimization: To determine the hyperplane's ideal weights, an optimization procedure is used.
4) Measurement and Interpretation: Measurement of the output of the quantum state and interpretation of the final decision plane is carried out.

The optimization problem in QSVC is identical to that of a classical SVC, but it utilizes a quantum kernel. The expression representing the general SVC optimization problem is given by (1).

$$\min_{w,b} ||w||^2 \text{ such that } y_i\,(wx_i + b) \geq 1, i = 1, \ldots, N \quad (1)$$

where x_i is a data point and y_i is the corresponding label 1 or -1. w and b denote the weights and biases used respectively.

To allow for some data points to be misclassified or to account for the data not being linearly separable, a slack variable ξ is first introduced with a weight C that controls the trade-off between maximisation of the margin and minimization of the classification error for each training instance as shown in (2).

$$\min_{w,b,\xi_i>0} ||w||^2 + C\sum_{i=1}^{N} \xi_i$$
$$\text{such that } y_i\,(wx_i + b) \geq 1 - \xi_i, \quad i = 1, \ldots, N \quad (2)$$

The term $C\sum_{i=1}^{N} \xi_i$ denotes the overall penalty for misclassification by the SVC.

Combining $\xi \geq 0$ and $y_i\,(wx_i + b) \geq 1 - \xi_i$, the optimization problem can be rewritten as (3).

$$\min_{w,b,\xi_i>0} ||w||^2 + C\sum_{i=1}^{N} \max\,(0, 1 - y_i\,(wx_i + b)) \quad (3)$$

In (3), the hinge loss is represented by the second term, which is a measurement of the distance between the actual and predicted values. If the predicted value matches the actual

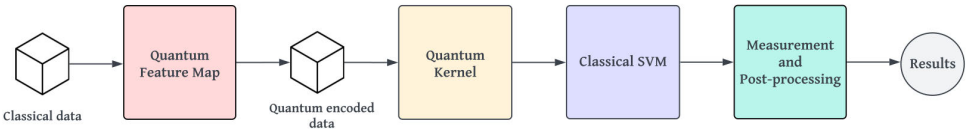

FIGURE 3. A general pipeline for QSVC.

value, the term tends to zero. If the value is non-zero, the difference between the actual and expected values and the loss are inversely related.

In optimization theory, a dual formulation is defined as an alternative representation of a given optimization problem that is equivalent to its primal formulation. The dual formulation is generally easier to solve than the primal formulation. The dual formulation of (3) is shown in (4).

$$\max_{\alpha_i} \sum_i -\frac{1}{2} \sum_{j,k} \alpha_j \alpha_k y_j y_k \left(x_j^T x_k\right) \quad \text{where } 0 \leq \alpha_i \leq C \text{ and } \sum_i \alpha_i y_i = 0 \tag{4}$$

This expression deals with calculating scalar products $x_j^T x_k$ between pairs of vectors. In order to maximize it, the data has to be linearly separable. Linear separability can be enforced by embedding the data in a higher dimensional space using a feature map. The scalar products can then be computed in the higher dimension.

Based on the feature map used, a kernel can calculate the scalar products without having to embed the data points, making the optimization process more efficient and less computationally intensive. Given two input vectors, it outputs their inner product in the transformed space. The kernel function which solves the optimization problem in QSVC is mathematically represented in (5),

$$K\left(\vec{x}, \vec{z}\right) = \left|\langle \phi\left(\vec{x}\right) | \phi\left(\vec{z}\right) \rangle\right| \tag{5}$$

where K is the quantum kernel function and $\phi(x)$ is the quantum feature map.

Quantum feature maps are quantum circuits that transform classical data into quantum states. Types offered by Qiskit [42] include ZFeatureMap, ZZFeatureMap, and PauliFeatureMap, among others. The quantum feature map employed in this work is a ZZFeatureMap using two qubits and two repeated circuits, as illustrated in Fig. 4. It exploits ZZ interactions between qubits to produce entanglement and effectively encode classical data.

Finally, the loss function minimized by QSVC by optimizing the parameters $\vec{\alpha}$ is represented in (6).

$$L(W) = \sum_i \alpha_i - \frac{1}{2} \sum_{i,j} y_i y_j \alpha_i \alpha_j K\left(\vec{x_i}, \vec{x_j}\right) \tag{6}$$

The experiment was carried out using a quantum kernel instantiated with the Aer simulator statevector backend provided by Qiskit. A one-vs-rest scheme was employed implicitly by scikit-learn [43] SVC to facilitate the multi-class classification.

B. MULTICLASS PEGASOS QUANTUM SUPPORT VECTOR CLASSIFIER

Primarily derived from [44], the Pegasos algorithm is an effective and scalable technique for solving the quadratic SVM problem. The Pegasos algorithm fundamentally employs a sub-gradient descent method for optimization. The objective of the algorithm is to identify a hyperplane that separates the two classes under consideration until the cost function described in Eq. (1) is minimized. The hybrid quantum model evolved from the above for classification tasks is known as the Pegasos QSVC.

The Pegasos algorithm is initialized with a solution that is iteratively improved by moving in the opposite direction of the objective function's negative gradient. Each iteration is responsible for the updation of the weight vector ẃánd the bias b́ón a mini-batch of data. To ensure convergence to the ideal value, the approach uses a step size that is inversely proportional to the number of repetitions.

The technique then uses the kernel approach to solve the quadratic optimization problem to determine the best boundary in this higher dimensional space [45]. The Pegasos QSVC implements the kernel equation represented in (5), and runs in a time complexity independent of the training set size.

The scope of the Pegasos QSVC is currently limited to binary classification tasks. Work has been done to incorporate multiclass classification on SVMs by using combinations of binary classification algorithms. In [46], the authors employ an Adaptive Binary Tree (ABT). The proposed solution concentrates on locally choosing the minimal number of Support Vectors(SVs) per classification. The authors in [47] propose an implementation by limiting the number of hyperplanes used in the standard one-against-one technique.

The proposed implementation applies combinatoric mathematics. The number of combinations possible for four classes taken two at a time is six. Feature extraction is carried out as mentioned in Section IV-A1.

The next step before training the proposed model is separating data into groups of classes: *NP*, *AH*, *MI*, and *H. MI* for features and labels separately. After which, each feature and label group is split into train and test sets in the ratio of 80:20. Consequently, the train and test sets for each pair of classes is generated by merging the corresponding train and test sets. Once combined, the features and labels of the train set for each pair of classes are shuffled to allow for homogeneity across all the combinations.

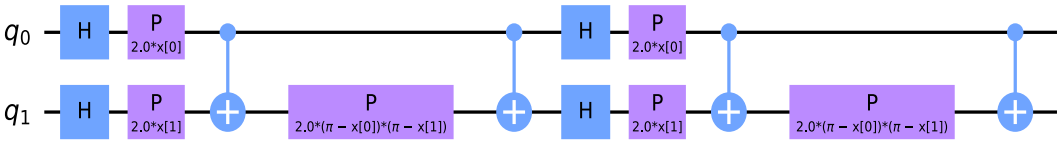

FIGURE 4. Circuit representing the ZZFeatureMap with two qubits and two circuit repetitions as employed in this work.

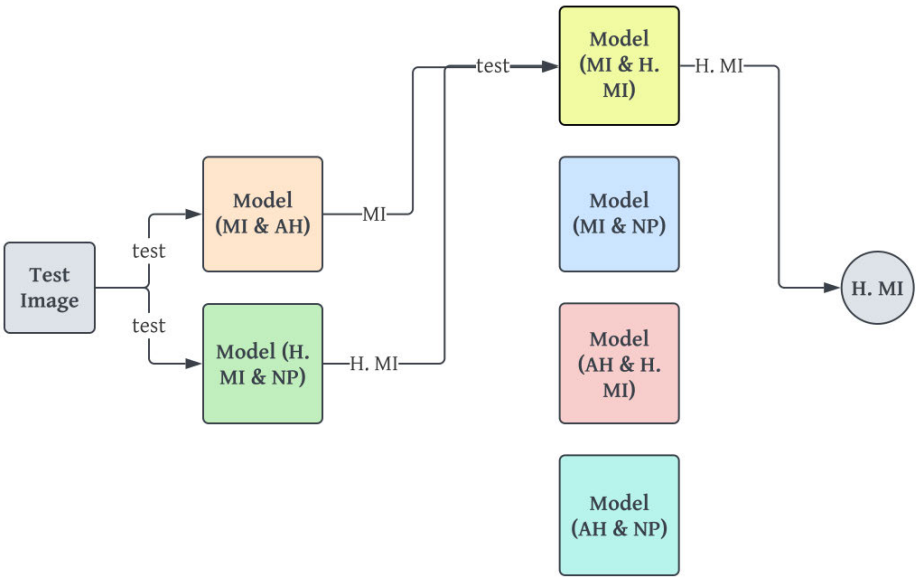

FIGURE 5. Pipeline followed for Multiclass Pegasos QSVC.

An individual Pegasos QSVC model in the proposed approach consists of three integral hyperparameters, specifically, the number of features which is considered as 9, the positive regularization parameter C, which is used to monitor the loss incurred and avoid underfitting as well as overfitting, and the number of steps τ, taken during the training process.

Since one model does not suffice for all 4 classes, 6 binary models are trained using corresponding pairs of train sets and hyperparameters. The quantum kernel employed for the model generation is as mentioned in Section IV-A2.

Algorithm 1 represents the multiclass approach applied to the binary Pegasos QSVC. In the algorithm, $model_{xy}$ represents a Pegasos model trained on classes x and y. The test() represents a function that takes a model and a test image as arguments and returns the result of testing the model with the given image.

To classify a test image in the proposed framework, it is first passed through two of the models. Depending on the classes predicted by the two models, the test image is then passed through a third model which is trained on the two predicted classes. The prediction from the third model is taken as the final prediction for the test image. Thus the proposed approach achieves multi-class classification with Pegasos QSVC.

To illustrate the approach, consider an image of class *H. MI* as seen in Fig. 5. To begin with, it is passed through two models trained on different pairs of classes, namely, *MI & AH* and *H. MI & NP*. Using the figure as a reference, the outputs of the models are *MI* and *H.MI* respectively. Consequently, the test image is then passed through the model trained on

Algorithm 1 Multiclass Pegasos QSVC Algorithm

Input: *test_image*
Output: $pred_{final}$
$pred_{01} \leftarrow$ test($model_{01}$, *test_image*)
$pred_{23} \leftarrow$ test($model_{23}$, *test_image*)
if $pred_{01} == 0$ **then**
  if $pred_{23} == 2$ **then**
    $pred_{final} \leftarrow$ test($model_{02}$, *test_image*)
  else
    $pred_{final} \leftarrow$ test($model_{03}$, *test_image*)
  end if
else
  if $pred_{23} == 2$ **then**
    $pred_{final} \leftarrow$ test($model_{12}$, *test_image*)
  else
    $pred_{final} \leftarrow$ test($model_{13}$, *test_image*)
  end if
end if
return $pred_{final}$

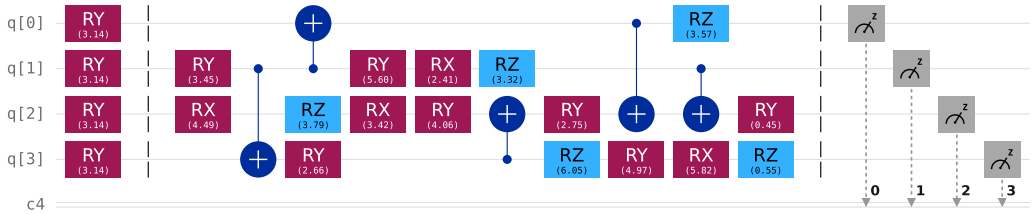

FIGURE 6. Circuit employed for the quantum layer of QNN.

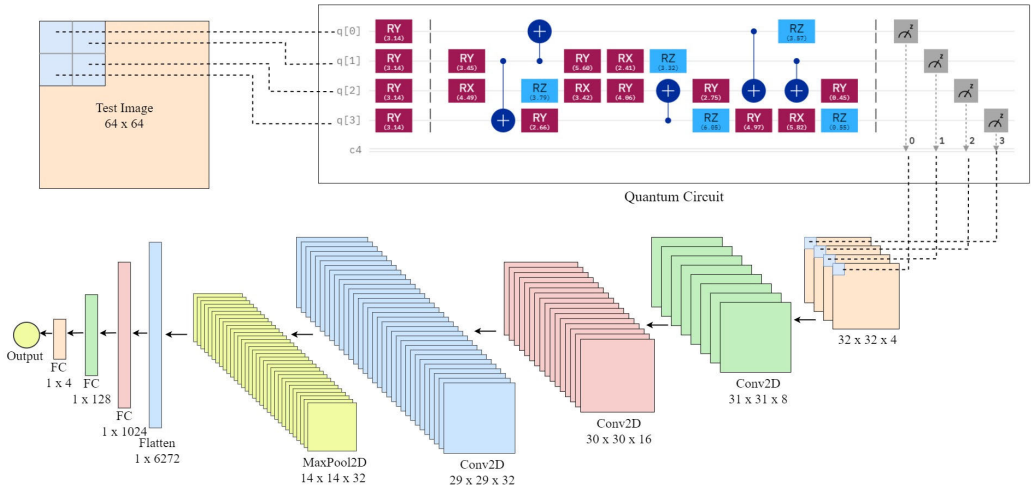

FIGURE 7. Proposed QNN architecture.

the *MI* and *H. MI* classes. This model then produces the final prediction as *H. MI*.

C. QUANVOLUTIONAL NEURAL NETWORK (QNN)

The motivation to integrate CNNs [48] with quantum layers arises from an effort to enhance the capabilities of these networks. CNNs are able to process and classify visual data owing to their ability to extract hierarchical features. Introducing quantum layers [49], is an innovative step in enhancing a CNN as it represents a new kind of transformational layer that integrates quantum computing in the traditional architecture. Thus the network can perform local transformations on the data using quantum circuits. These quantum circuits offer new avenues for feature extraction.

The work in [49] described the Quanvolutional model's ability to leverage random nonlinear features, modify training time, and model complex relationships using computational resources at polynomial time complexity. This combination makes the Quanvolutional model an excellent choice to consider for image classification problems.

1) DESIGN OF QUANTUM FILTER

In the quanvolutional approach, the input data is transformed using quantum circuits instead of the classical matrix operations. The specific quantum circuit, as depicted in Fig. 6, is composed of a series of quantum gates, including R_x, R_y, R_z (which are rotation gates acting on different axes of the Bloch sphere), CNOT, and Pauli-Z measurement gates. The quantum gates employed, their notation, and operations are expanded upon in Table 1.

2) IMPLEMENTATION

Images were resized to dimensions of 64 × 64 pixels. Subsequently, the images were divided into square subregions of dimension 2 × 2, which were passed to the quantum circuit iteratively. Quantum operations are performed on the input according to the circuit. Four values are returned which are then stacked as individual pixels on different channels, thereby transforming the input to a dimension of 32 × 32x4. The proposed QNN architecture is shown in Fig.7.

After applying the quantum convolutional layer, the resulting features are then fed into the proposed CNN architecture. The proposed 8-layered CNN architecture comprises of three 2D convolutional layers employed with the ReLU activation function, a max pooling layer, a flatten layer, and 3 fully connected layers. The first convolutional layer contains 8 filters which are doubled across each of the next two layers. The filter size chosen is 2 × 2, with a stride of 1.

Subsequently, a max pooling layer is employed with a pool size of 2 × 2. The features are flattened and further passed to three fully connected layers. The 1024 nodes make up the first completely connected layer, which is followed by

TABLE 2. Model parameters QNN.

Layer	Units	Output size	Number of Parameters
Quantum Conv2d	4	32x32x4	0
Conv2d	8	31x31x8	136
Conv2d	16	30x30x16	528
Conv2d	32	29x29x32	2080
MaxPool2d	-	14x14x32	0
Flatten	-	6272	0
Dense	1024	1024	6423552
Dense	128	128	131200
Dense	4	4	516

Total trainable parameters: 6,558,012

TABLE 3. Evaluation metrics.

Metric	Formula
Accuracy (Acc.)	$\frac{TP+TN}{TP+TN+FP+FN}$
Precision (Prc.)	$\frac{TP}{TP+FP}$
Recall (Rec.)	$\frac{TP}{TP+FN}$
F1-Score (F1)	$2 \cdot \frac{Precision \cdot Recall}{Precision + Recall}$
Specificity (Spc.)	$\frac{TN}{TN+FP}$

TP = True Positive; TN = True Negative;
FP = False Positive; FN = False Negative.

a layer of 128 nodes. The final layer comprises of 4 nodes with softmax activation function, thus making it suitable for multi-class classification of four classes. This has been summarized in Table 2.

V. RESULTS AND DISCUSSION

Model performances have been evaluated using the metrics listed in Table 3.

Proceeding to the QNN, the number of layers for the quantum circuit was chosen to be four after comparing results with other values. The results of the simulations are illustrated in Fig. 9.

A. HYPERPARAMETER TUNING

Appropriate tuning of hyperparameters can lead to significant enhancement in the model performance. The number of features fed into the QSVC model, also corresponding to the number of qubits used by the model, is a critical point of discussion. The corresponding accuracies obtained by varying it within a range of 2 to 18 are depicted in Fig. 8. The graph followed an increasing trend till n = 7, post which minor variations are observed until n = 13. Subsequently, the graph stabilized to a constant value. The maximum accuracy of 94.09% is observed at n = 9, hence the optimal choice for the model.

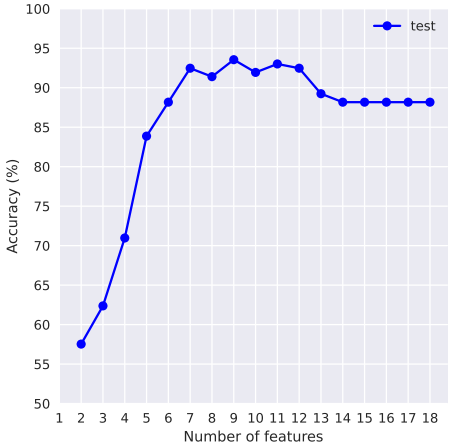

FIGURE 8. Experimental results for number of features vs accuracy for QSVC.

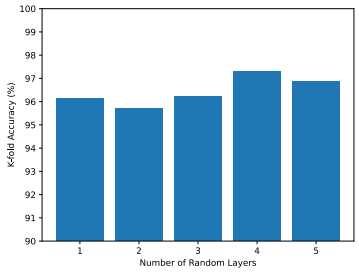

FIGURE 9. Experimental results for number of random layers vs K-fold accuracy for QNN.

To maintain uniformity, the Pegasos QSVC models' feature input was set at 9 features. The regularization parameter (C) and number of repetitions (τ) were tuned for each of the 6 binary models. The model evaluation parameters and the hyperparameters for each model are displayed in Table 4.

B. COMPARATIVE ANALYSIS AND DISCUSSION

We highlight significant results from the experiments in this section. The SVC plays a crucial role in machine learning research owing to its high accuracy in classification tasks, flexibility, robustness, interpretability, and efficiency. These characteristics enable it to function as a good baseline algorithm in machine learning research, where the goal is to

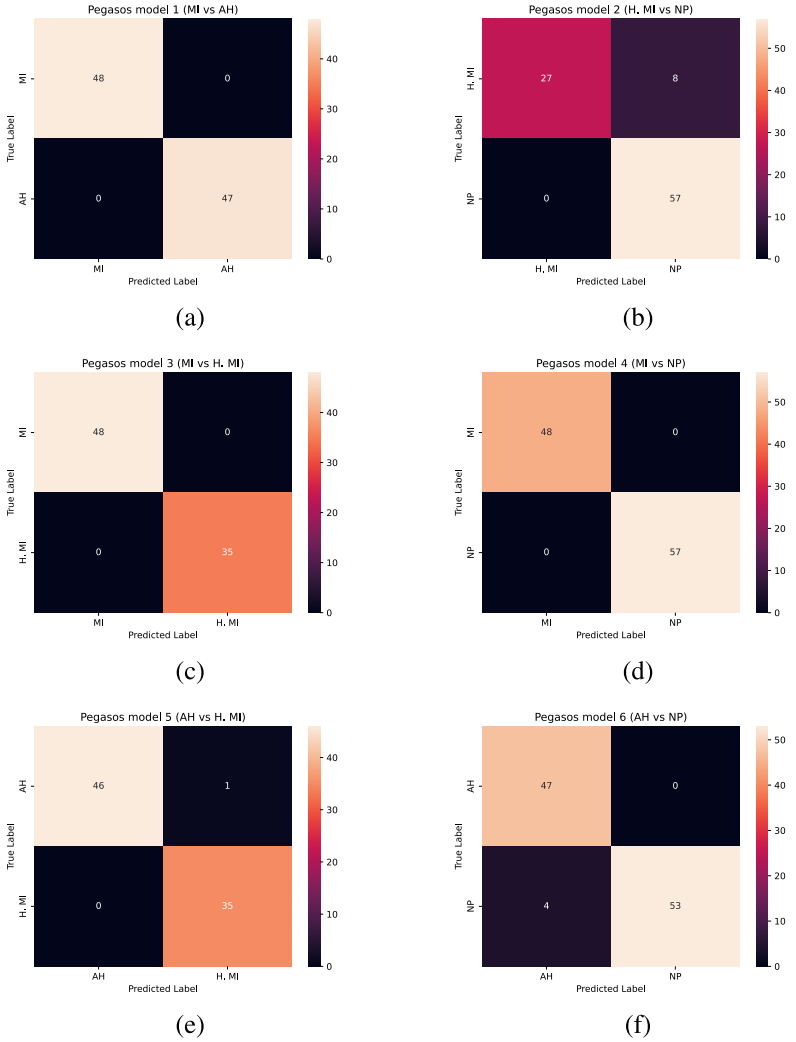

FIGURE 10. Confusion matrices of individual Multiclass Pegasos QSVC models (a) MI vs AH (b) H. MI vs NP (c) MI vs H. MI (d) MI vs NP (e) AH vs H. MI (f) AH vs NP.

TABLE 4. Performance measures of individual binary classifiers in Multiclass Pegasos QSVC.

Model	C	τ	Acc. (%)	Prc. (%)	Rec. (%)	F1 (%)	Spc. (%)	t (s)
MI vs AH	1200	1000	100.00	100.00	100.00	100.00	100.00	2170.55
MI vs H. MI	1200	1000	100.00	100.00	100.00	100.00	100.00	1936.54
MI vs NP	1200	1000	100.00	100.00	100.00	100.00	100.00	2084.92
AH vs H. MI	1200	2500	98.78	97.22	100.00	98.59	100.00	9090.58
AH vs NP	1400	2000	96.15	100.00	92.98	96.36	92.98	7569.10
H. MI vs NP	1400	2000	91.30	87.69	100.00	93.44	100.00	7092.69

develop techniques that can outperform it. The performance measures of SVC are shown in Table 6.

Table 6 shows that the QSVC outperformed the SVC by +10.76% accuracy, +9.73% precision, +10.76% recall, +10.79% F1 score, and +3.73% specificity respectively.

The results of the binary Pegasos QSVC models are summarized in Table 4. Fig. 10 demonstrates the confusion matrices for each model. The proposed implementation enabling multiclass Pegasos classification performed comparably to QSVC as per the results depicted

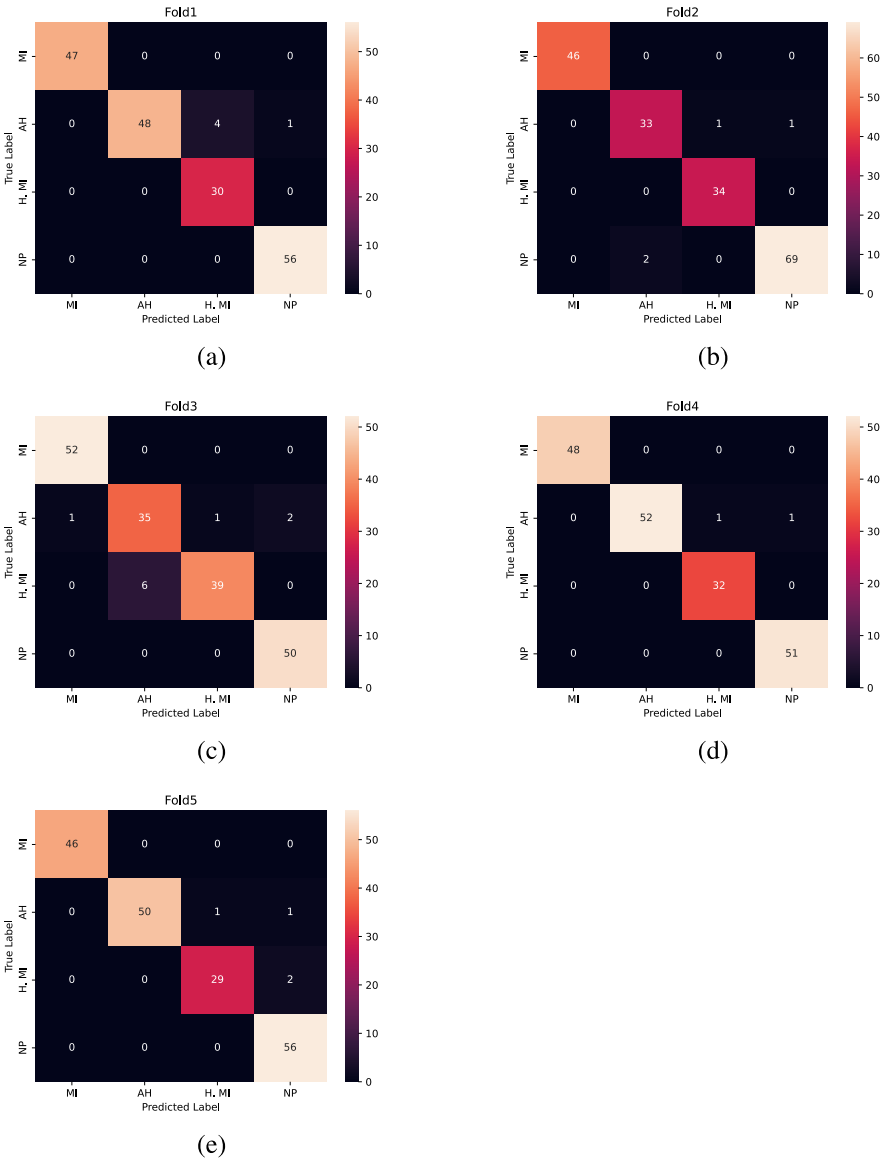

FIGURE 11. Fold-wise confusion matrices of QNN (a) Fold 1 (b) Fold 2 (c) Fold 3 (d) Fold 4 (e) Fold 5.

TABLE 5. Fold-wise performance of QNN.

Fold	Acc. (%)	Prc. (%)	Rec. (%)	F1 (%)	Spc. (%)	t (s)
Fold-1	97.31	97.57	97.31	97.31	99.10	323.63
Fold-2	97.85	97.86	97.85	97.85	99.28	383.08
Fold-3	94.62	94.77	94.62	94.59	98.21	383.44
Fold-4	98.92	98.95	98.92	98.92	99.64	383.10
Fold-5	97.84	97.90	97.84	97.84	99.28	364.03
Aggregate	**97.31**	**97.41**	**97.31**	**97.30**	**99.10**	**364.03**
	±1.44	**±1.40**	**±1.44**	**±1.45**	**±0.48**	**±23.14**

in Table 6 and the final confusion matrices displayed in Fig. 12.

The proposed QNN implementation obtained an accuracy of 97.31%, precision of 97.41%, recall value of 97.31%, F1 score of 97.30%, and specificity of 99.10%, as represented in Table 6. Moreover, the table also shows that the QNN outperformed its classical CNN counterpart by +3.88% accuracy, +3.73% precision, +3.88% recall, +3.97% F1 score, and +1.29% specificity, with the CNN derived by removing the quantum layer from the QNN architecture given in 7. The results were validated using 5-fold cross-validation. Detailed fold-wise metrics are displayed in

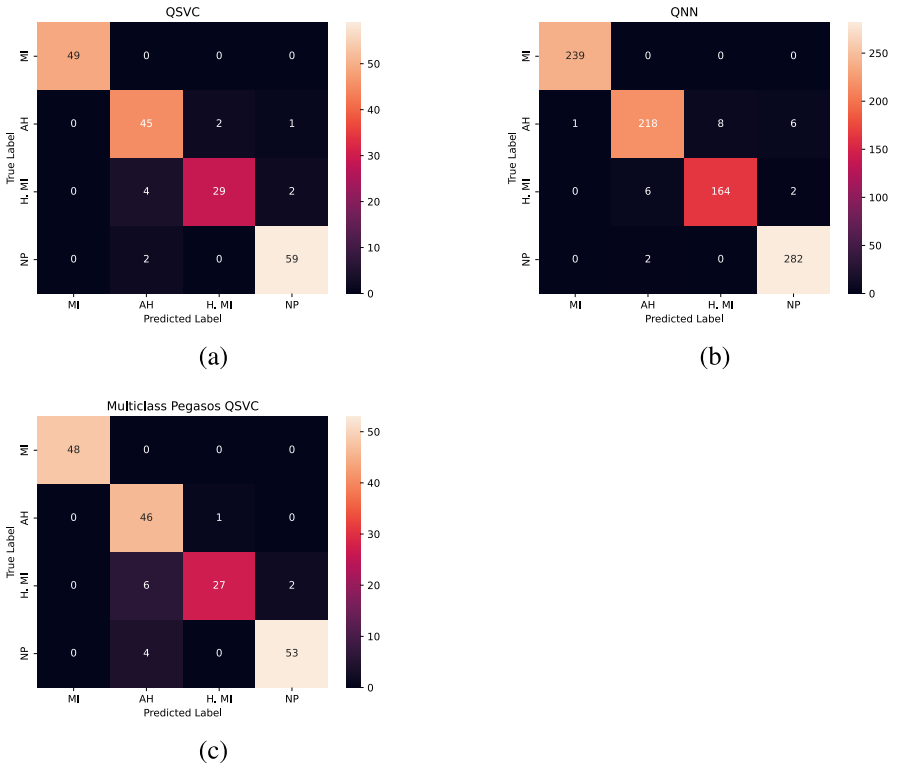

FIGURE 12. Final confusion matrices of the models presented (a) QSVC (b) QNN (c) Multiclass Pegasos QSVC .

TABLE 6. Performance measures of SVC, QSVC, Pegasos QSVC, CNN, and QNN.

Model	Acc.(%)	Prc.(%)	Rec.(%)	F1.(%)	Spc.(%)
SVC [38]	83.33	84.43	83.33	83.25	94.25
QSVC [37]	94.09	94.16	94.09	94.04	97.98
Proposed Multiclass Pegasos QSVC	93.05	93.74	93.05	93.01	97.66
CNN	93.43	93.68	93.43	93.33	97.81
Proposed QNN	**97.31**	**97.41**	**97.31**	**97.30**	**99.10**

TABLE 7. General Comparison of QPSO-SVM and QNN.

Model	Acc.(%)	Prc.(%)	Rec.(%)	F1.(%)	Spc.(%)
QPSO-SVM [50]	96.31	94.23	96.13	95	93.56
Proposed QNN	**97.31**	**97.41**	**97.31**	**97.30**	**99.10**

Table 5. Fig. 11 displays the confusion matrices for each fold. The results from the table show that the performance of each fold is comparable to the other folds and they display a minimal standard deviation. The confusion matrix obtained by summing up those of the folds is displayed in Fig. 12. Compared to the QSVC model, the QNN exhibited an increase in accuracy of +3.22%, precision of +3.25%, recall score of +3.22%, F1 score of +3.26%, and specificity of +1.12%. In comparison to the proposed Multiclass Pegasos QSVC model, the QNN exhibited an increase in accuracy of +4.26%, precision of +3.67%, recall score of +4.26%, F1 score of +4.29%, and specificity of +1.44%. Hence, the QNN is the best-performing model.

We draw a few conclusions from the confusion matrices in Fig. 10, Fig. 11, and Fig. 12. The trend in misclassification of a particular class as another class is consistent across all the models. Images of the *MI* class are never misclassified, indicating they are easily distinguishable. Whenever an *NP* class image gets miscategorized, it is with the *AH* class. An *H. MI* class image is never misclassified as an *MI* class image. An *AH* class image is more likely to get misclassified as that of *H. MI* or *NP* than that of *MI*.

In general, we have compared our proposed QNN method with cardiovascular disease classification using quantum particle swarm optimization and support vector machine (QPSO-SVM) [50] in Table 7. Our method performs better

in terms of Accuracy, Precision, Recall, F1 Score and Specificity.

The QNN takes a streamlined approach, employing a simple state simulator of qubit-based quantum circuit architecture via Pennylane in a four-qubit configuration. The QSVC and Pegasos QSVC, on the other hand, use the Aer simulator within the experimental setup, providing a computational foundation for their quantum processing.

This distinction highlights the tradeoff inherent in the quantum architectures used between computational complexity and quantum technology used. The QNN prioritizes simplicity with its minimalistic quantum circuit configuration, potentially facilitating ease of implementation and interpretation. The QSVC and Pegasos QSVC, on the other hand, may offer enhanced computational capabilities at the cost of increased complexity by utilizing the Aer simulator.

VI. CONCLUSION AND FUTURE SCOPE

In this work, we have successfully presented the application of QML for the multi-class classification of CVDs using ECG images. The paper demonstrated the potential of QML models to outperform classical models. The work proved the ability to perform multi-class classification by illustrating the same with the application of combinatoric mathematics on the Pegasos QSVC model. The proposed QNN implementation presented in this study performed exceptionally well. Post the NISQ era, quantum algorithms are bound to be significantly more powerful. Thus, future prospects in the field are promising. Advancement in this field could comprise of integrating QML models with quantum hardware and incorporating the same within existing medical systems can help improve diagnostics. The development of QML models can aid in the early detection and prediction of more medical ailments and thus help save lives.

ACKNOWLEDGMENT

The authors acknowledge the use of IBM quantum services.

REFERENCES

[1] C. W. Tsao, A. W. Aday, Z. I. Almarzooq, A. Alonso, A. Z. Beaton, M. S. Bittencourt, A. K. Boehme, A. E. Buxton, A. P. Carson, Y. Commodore-Mensah, and M. S. Elkind, "Heart disease and stroke statistics—2022 update: A report from the American heart association," *Circulation*, vol. 145, no. 8, pp. 153–639, 2022.

[2] A. R. Kim, J. Y. Kim, K. Choi, and D. S. Chung, "On-chip immunoassay of a cardiac biomarker in serum using a polyester-toner microchip," *Talanta*, vol. 109, pp. 20–25, May 2013.

[3] Z. Altintas, W. M. Fakanya, and I. E. Tothill, "Cardiovascular disease detection using bio-sensing techniques," *Talanta*, vol. 128, pp. 177–186, Oct. 2014. [Online]. Available: https://www.sciencedirect.com/science/article/pii/S0039914014003385

[4] T.-I. Yin, Y. Zhao, J. Horak, H. Bakirci, H.-H. Liao, H.-H. Tsai, Y.-Z. Juang, and G. Urban, "A micro-cantilever sensor chip based on contact angle analysis for a label-free troponin I immunoassay," *Lab Chip*, vol. 13, no. 5, p. 834, 2013. [Online]. Available: https://www.scopus.com/inward/record.uri?eid=2-s2.0-84875830922&doi=10.1039%2fc2lc40767a&partnerID=40&md5=5a6229418b2eee61386136902c22bfbd

[5] P. Mathur, S. Srivastava, X. Xu, and J. L. Mehta, "Artificial intelligence, machine learning, and cardiovascular disease," *Clin. Med. Insights, Cardiol.*, vol. 14, pp. 1–9, Sep. 2020.

[6] S. I. Ayon, M. M. Islam, and M. R. Hossain, "Coronary artery heart disease prediction: A comparative study of computational intelligence techniques," *IETE J. Res.*, vol. 68, no. 4, pp. 2488–2507, Jul. 2022.

[7] N. C. Thompson, K. Greenewald, K. Lee, and G. F. Manso, "The computational limits of deep learning," 2020, *arXiv:2007.05558*.

[8] S. Boixo, S. V. Isakov, V. N. Smelyanskiy, R. Babbush, N. Ding, Z. Jiang, M. J. Bremner, J. M. Martinis, and H. Neven, "Characterizing quantum supremacy in near-term devices," *Nature Phys.*, vol. 14, no. 6, pp. 595–600, Jun. 2018.

[9] T. Hey, "Quantum computing: An introduction," *Comput. Control Eng. J.*, vol. 10, no. 3, pp. 105–112, Jun.1999.

[10] R. Ur Rasool, H. F. Ahmad, W. Rafique, A. Qayyum, J. Qadir, and Z. Anwar, "Quantum computing for healthcare: A review," *Future Internet*, vol. 15, no. 3, p. 94, Feb. 2023.

[11] R. Orús, S. Mugel, and E. Lizaso, "Quantum computing for finance: Overview and prospects," *Rev. Phys.*, vol. 4, Nov. 2019, Art. no. 100028.

[12] P. Rebentrost and S. Lloyd, "Quantum computational finance: Quantum algorithm for portfolio optimization," 2018, *arXiv:1811.03975*.

[13] A. Ganapathy and A. Systems, "Quantum computing in high frequency trading and fraud detection," *Eng. Int.*, vol. 9, no. 2, pp. 61–72, 2021.

[14] J. Preskill, "Quantum computing in the NISQ era and beyond," *Quantum*, vol. 2, p. 79, Aug. 2018.

[15] K. Naja, S. F. Yelin, and X. Gao, "The development of quantum machine learning," Tech. Rep., 2022, doi: 10.1162/99608f92.5a9fd72c.

[16] S. Chakraborty, T. Das, S. Sutradhar, M. Das, and S. Deb, "An analytical review of quantum neural network models and relevant research," in *Proc. 5th Int. Conf. Commun. Electron. Syst. (ICCES)*, Jun. 2020, pp. 1395–1400.

[17] A. Kamruzzaman, Y. Alhwaiti, A. Leider, and C. C. Tappert, "Quantum deep learning neural networks," in *Advances in Information and Communication*, vol. 2. Berlin, Germany: Springer, 2020, pp. 299–311.

[18] N. Mathur, J. Landman, Y. Yvonna Li, M. Strahm, S. Kazdaghli, A. Prakash, and I. Kerenidis, "Medical image classification via quantum neural networks," 2021, *arXiv:2109.01831*.

[19] X. Gao, Z.-Y. Zhang, and L.-M. Duan, "A quantum machine learning algorithm based on generative models," *Sci. Adv.*, vol. 4, no. 12, Dec. 2018, Art. no. eaat9004, doi: 10.1126/sciadv.aat9004.

[20] J. R. McClean, J. Romero, R. Babbush, and A. Aspuru-Guzik, "The theory of variational hybrid quantum-classical algorithms," *New J. Phys.*, vol. 18, no. 2, Feb. 2016, Art. no. 023023.

[21] A. Matic, M. Monnet, J. M. Lorenz, B. Schachtner, and T. Messerer, "Quantum-classical convolutional neural networks in radiological image classification," in *Proc. IEEE Int. Conf. Quantum Comput. Eng. (QCE)*, Sep. 2022, pp. 56–66.

[22] A. Tariq Jamal, A. Ben Ishak, and S. Abdel-Khalek, "Tumor edge detection in mammography images using quantum and machine learning approaches," *Neural Comput. Appl.*, vol. 33, no. 13, pp. 7773–7784, Jul. 2021.

[23] K. Sengupta and P. R. Srivastava, "Quantum algorithm for quicker clinical prognostic analysis: An application and experimental study using CT scan images of COVID-19 patients," *BMC Med. Informat. Decis. Making*, vol. 21, no. 1, pp. 1–14, Dec. 2021.

[24] E. Acar and I. Yilmaz, "COVID-19 detection on IBM quantum computer with classical-quantum transferlearning," *Turkish J. Electr. Eng. Comput. Sci.*, vol. 29, no. 1, pp. 46–61, 2021.

[25] H. Gupta, H. Varshney, T. K. Sharma, N. Pachauri, and O. P. Verma, "Comparative performance analysis of quantum machine learning with deep learning for diabetes prediction," *Complex Intell. Syst.*, vol. 8, no. 4, pp. 3073–3087, Aug. 2022.

[26] D. Maheshwari, B. Garcia-Zapirain, and D. Sierra-Sosa, "Quantum machine learning applications in the biomedical domain: A systematic review," *IEEE Access*, vol. 10, pp. 80463–80484, 2022.

[27] L. Wei, H. Liu, J. Xu, L. Shi, Z. Shan, B. Zhao, and Y. Gao, "Quantum machine learning in medical image analysis: A survey," *Neurocomputing*, vol. 525, pp. 42–53, Mar. 2023.

[28] Y. Kumar, A. Koul, P. S. Sisodia, J. Shafi, K. Verma, M. Gheisari, and M. B. Davoodi, "Heart failure detection using quantum-enhanced machine learning and traditional machine learning techniques for Internet of Artificially Intelligent Medical Things," *Wireless Commun. Mobile Comput.*, vol. 2021, pp. 1–16, Dec. 2021.

[29] S. S. Kavitha and N. Kaulgud, "Quantum K-means clustering method for detecting heart disease using quantum circuit approach," *Soft Comput.*, vol. 27, no. 18, pp. 13255–13268, Sep. 2023.
[30] G. Abdulsalam, S. Meshoul, and H. Shaiba, "Explainable heart disease prediction using ensemble-quantum machine learning approach," *Intell. Autom. Soft Comput.*, vol. 36, no. 1, pp. 761–779, 2023.
[31] J. K. A. Das and M. Malhotra, "Quantum machine learning: An effective approach to high-dimensional learning," in *Proc. 6th Int. Conf. Comput. Syst. Inf. Technol. Sustain. Solutions (CSITSS)*, Dec. 2022, pp. 1–6.
[32] S. Alsubai, A. Alqahtani, A. Binbusayyis, M. Sha, A. Gumaei, and S. Wang, "Heart failure detection using instance quantum circuit approach and traditional predictive analysis," *Mathematics*, vol. 11, no. 6, p. 1467, Mar. 2023.
[33] D. Maheshwari, U. Ullah, P. A. O. Marulanda, A. G.-O. Jurado, I. D. Gonzalez, J. M. O. Merodio, and B. Garcia-Zapirain, "Quantum machine learning applied to electronic healthcare records for ischemic heart disease classification," *Hum.-Centric Comput. Inf. Sci.*, vol. 13, pp. 1–17, Feb. 2023.
[34] A. H. Khan, M. Hussain, and M. K. Malik, "ECG images dataset of cardiac and COVID-19 patients," *Data Brief*, vol. 34, Feb. 2021, Art. no. 106762.
[35] C. Antzelevitch and A. Burashnikov, "Overview of basic mechanisms of cardiac arrhythmia," *Cardiac Electrophysiol. Clinics*, vol. 3, no. 1, pp. 23–45, Mar. 2011.
[36] E. Boersma, N. Mercado, D. Poldermans, M. Gardien, J. Vos, and M. L. Simoons, "Acute myocardial infarction," *Lancet*, vol. 361, no. 9360, pp. 847–858, 2003.
[37] P. Rebentrost, M. Mohseni, and S. Lloyd, "Quantum support vector machine for big data classification," *Phys. Rev. Lett.*, vol. 113, no. 13, pp. 1–15, Sep. 2014.
[38] B. E. Boser, I. M. Guyon, and V. N. Vapnik, "A training algorithm for optimal margin classifiers," in *Proc. 5th Annu. Workshop Comput. Learn. Theory*, Jul. 1992, pp. 144–152.
[39] K. He, X. Zhang, S. Ren, and J. Sun, "Deep residual learning for image recognition," in *Proc. IEEE Conf. Comput. Vis. Pattern Recognit. (CVPR)*, Jun. 2016, pp. 770–778.
[40] J. Deng, W. Dong, R. Socher, L.-J. Li, K. Li, and L. Fei-Fei, "ImageNet: A large-scale hierarchical image database," in *Proc. IEEE Conf. Comput. Vis. Pattern Recognit.*, Jun. 2009, pp. 248–255.
[41] F. Pedregosa, G. Varoquaux, A. Gramfort, V. Michel, B. Thirion, O. Grisel, M. Blondel, P. Prettenhofer, R. Weiss, V. Dubourg, and J. Vanderplas, "Scikit-learn: Machine learning in Python," *J. Mach. Learn. Res.*, vol. 12, pp. 2825–2830, Feb. 2011. [Online]. Available: https://scikit-learn.org
[42] Qiskit Contributors. (2023). *Qiskit: An Open-Source Framework for Quantum Computing*. Accessed: Apr. 15, 2023. [Online]. Available: https://qiskit.org
[43] L. Buitinck, G. Louppe, M. Blondel, F. Pedregosa, A. Mueller, O. Grisel, V. Niculae, P. Prettenhofer, A. Gramfort, J. Grobler, and R. Layton, "API design for machine learning software: Experiences from the scikit-learn project," in *Proc. ECML PKDD Workshop: Lang. Data Mining Mach. Learn.*, 2013, pp. 108–122.
[44] S. Shalev-Shwartz, Y. Singer, and N. Srebro, "Pegasos: Primal estimated sub-gradient solver for SVM," in *Proc. 24th Int. Conf. Mach. Learn.*, Jun. 2007, pp. 807–814.
[45] C. Blank, D. K. Park, J.-K.-K. Rhee, and F. Petruccione, "Quantum classifier with tailored quantum kernel," *npj Quantum Inf.*, vol. 6, no. 1, pp. 1–7, May 2020.
[46] J. Chen, C. Wang, and R. Wang, "Adaptive binary tree for fast SVM multiclass classification," *Neurocomputing*, vol. 72, pp. 3370–3375, Aug. 2009. [Online]. Available: https://www.sciencedirect.com/science/article/pii/S0925231209001106
[47] R. Debnath, N. Takahide, and H. Takahashi, "A decision based one-against-one method for multi-class support vector machine," *Pattern Anal. Appl.*, vol. 7, no. 2, pp. 164–175, Jul. 2004.
[48] K. O'Shea and R. Nash, "An introduction to convolutional neural networks," 2015, *arXiv:1511.08458*.
[49] M. Henderson, S. Shakya, S. Pradhan, and T. Cook, "Quanvolutional neural networks: Powering image recognition with quantum circuits," *Quantum Mach. Intell.*, vol. 2, no. 1, pp. 1–9, Jun. 2020.
[50] E. I. Elsedimy, S. M. M. AboHashish, and F. Algarni, "New cardiovascular disease prediction approach using support vector machine and quantum-behaved particle swarm optimization," *Multimedia Tools Appl.*, pp. 1–28, Aug. 2023, doi: 10.1007/s11042-023-16194-z.

SHARANYA PRABHU is currently pursuing the B.Tech. degree in computer science and engineering with the Manipal Institute of Technology, Manipal, Karnataka, India. She was a Machine Learning Engineering Intern with Trikaiser and as a Software Developer Intern with Fidelity Investments. Her current research interests include quantum machine learning, machine learning, artificial intelligence, and data streaming algorithms. She was a recipient of the Diamond Jubilee Award for CSE Branch Topper 2020–2021. She qualified for the Grand Finale of the QETCI Quantum Science and Technology Hackathon 2022 as one of the top 16 out of more than 1100 teams.

SHOURYA GUPTA is currently pursuing the B.Tech. degree in computer science and engineering with the Manipal Institute of Technology, Manipal, Karnataka, India.

He was a Research Intern with the Medical Imaging and Theranostics Laboratory, Indian Institute of Technology, Kharagpur, working in the domain of medical AI. He was a Software Engineering Intern with SAP Labs India. He qualified for the finals of the QETCI Quantum Science and Technology Hackathon 2022, being part of one of the Top 16 teams out of more than 1100 participating teams from 25 different countries. His research interests include applied machine learning, deep learning, and quantum machine learning.

GAUTHAM MANURU PRABHU is currently pursuing the B.Tech. degree in computer science engineering with the Manipal Institute of Technology, Manipal, Karnataka, India.

He was a Research Intern with the Medical Informatics Laboratory, Indian Institute of Technology, Kharagpur. He qualified for the grand finale of the QETCI Quantum Science and Technology Hackathon 2022 as one of the top 16 out of more than 1100 teams from 25 different countries. His research interests include the applications of machine learning, quantum machine learning for enhanced informatics, and optimization problems.

AARUSHI VISHAL DHANUKA is currently pursuing the B.Tech. degree in computer and communication engineering with the Manipal Institute of Technology, Manipal, Karnataka, India. She was a Research Intern with the Jawaharlal Nehru Centre for Advanced Scientific Research. Her research interests include quantum computing and its multifaceted applications and solutions, machine learning, data analysis, as well as their integration into enhanced informatics and optimization problems.

K. VIVEKANANDA BHAT (Senior Member, IEEE) received the Ph.D. degree in computer science and engineering from IIT Kharagpur, India, and the M.Tech. degree in systems analysis and computer applications from the National Institute of Technology Karnataka, Surathkal, India. He is currently an Additional Professor with the Department of Computer Science and Engineering, Manipal Institute of Technology, Manipal Academy of Higher Education, Manipal, India. He has published several articles in reputed Web of Science indexed international journals and conferences. His research interests include quantum computing and cyber security.